

Challenges of PV Integration in Low-Voltage Secondary Networks

P. Mohammadi, *Student Member, IEEE*, S. Mehraeen, *Member, IEEE*

Abstract— This paper presents challenges and potential impacts of Photovoltaic (PV) integration in the low-voltage downtown secondary networks (downtown networks). In the conventional secondary networks, substation feeders are the sole source of electric power and establish unidirectional power to the downtown network. The network protectors prevent the flow of power from inside the network to the upstream feeder by disconnecting the circuit to protect the feeder transformer against upstream faults. The assumption of unidirectional power flow can be violated by PV generation due to the possibility of excess power inside the network. It is shown in this paper that a large number of network protector trips can occur, and thus voltage collapse may follow even in low PV penetration levels. In addition, it is demonstrated that the reclose action of the network protector relays is adversely affected by the PV power. Other adverse effects of such DG units, such as voltage profile, line overloads, and flicker, are also briefly discussed. Finally, a solution is proposed, based on differential currents, to upgrade the network protector relays in order to avoid false trips due to excess PV power. Part of the New Orleans downtown network is modeled and the study is performed through simulations.

Index Terms—Low-Voltage secondary network, Photovoltaic (PV), Distributed Generation (DG), Downtown network, Microprocessor Network Protector Relay (MNPR).

I. INTRODUCTION

Electric power systems have been experiencing fast and fundamental changes in recent years due to the introduction of distributed generation (DG). The smart grid, utilizing renewable energy-based distributed generation, attracts great attention due to environmental and reliability concerns [1], [2]. Government incentives, technological advances, and many other factors have resulted in a dramatic growth in photovoltaic (PV) power utilization and integration by both customers and utility companies [1]–[3]. Approximately 1.3 gigawatts of PV power were installed in the United States in the first quarter of 2015 resulting in a total of 21.3 GW of installed capacity [3]. The residential share of this installed capacity is 400 megawatts, which is a 76% rise compared to the same period in 2014 [3]. While this rapid pace of PV integration can potentially cause problems if not treated properly, both the government and utility customers have a great desire for PV integration.

Conventional urban lateral distribution networks are designed to accommodate unidirectional power flow from generation plants to the customers. This assumption is prone to

violation by PV units causing reverse power flow in the case of excess power generation. The bidirectional flow of power can potentially interfere with the protective equipment. Other network operational conditions such as voltage profile, flicker, etc., can also be affected by the presence of PV power [1], [2]. Cloud effect, weather unpredictability, sun irradiance hourly changes, uncertainties in PV operational conditions, losses due to improper integration, etc., can add additional challenges to the operation of the distribution networks [4], [5].

PV integration is more challenging in downtown underground networks than radial distribution networks due to the highly meshed circuit configuration and unidirectional power flow requirements. There exists very little research on PV power integration in low-voltage (LV) secondary networks especially when it comes to network protection [4]. Since integrated PV power generation was not considered in network designs, if customers install PV generators with capacity higher than their consumption, the networks safety and reliability can be compromised resulting in frequent outages, excessive overloading, and inability in fault current termination [1]–[6].

One of the impacts of PV power on the secondary network is the network protection malfunction. Excess PV power can lead to loss of coordination, changes in fault ratings and source contributions [8]–[11]. In addition, solar irradiance is not fully predictable resulting in intermittent power generation on cloudy days. This may affect the network voltage profile [4] and cause voltage flicker. Also, excessive PV power generation can cause overvoltage [7]. However, the most critical effect of the integration of PV power in downtown networks is the network protector false trip and reclose issues that can lead to reactive power shortage and voltage instability which are the main focus of this research.

In [4] the effects of inverter-based, induction, and synchronous DGs on the secondary network's voltage profiles are investigated and the possibility of over and under voltage are explored by using probabilistic DG power distribution. It is also mentioned in [4] that with DG penetration in the network there is a chance of network protector tripping. However, the undesirable network protector false tripping is not elaborated on in [4]. Indeed, incidents such as cascaded network protector trips, transformer overloads, and reclose issues are very likely in the presence of DG due to reverse power flow.

Authors are with the school of Electrical Engineering and Computer Science, Louisiana State University, Electrical Engineering Building, South Campus Dr., Baton Rouge, LA 70803. Contact authors: pmoham1@lsu.edu, smehraeen@lsu.edu.

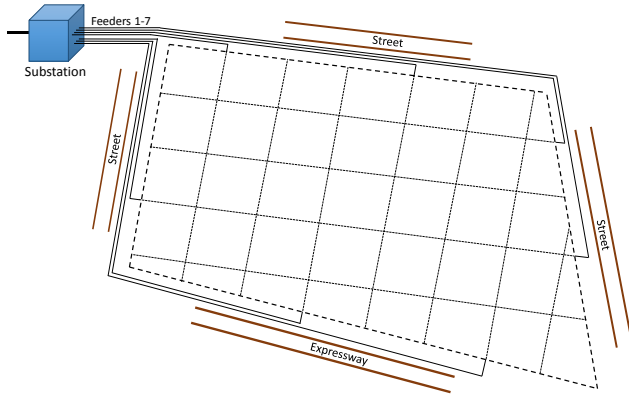


Fig. 1 Approximate street boundaries and schematic of the network

By contrast, this research focuses on the issue of reverse power flow and network protector false tripping and shows that widespread network protector trips and total secondary network voltage collapse can occur with low and moderate PV penetration levels. Much attention is paid to PV power rather than DG to address reactive power shortage, power variability, intermittence of power, and the emergence of the PV installments in downtown networks. The cascaded trips of network protectors can occur at some levels of PV penetration which may lead to shortage of reactive power from the primary feeders, and thus voltage instability. It is also shown here that the PV units can interfere with the reclose operation of the network protectors. These issues have not been fully investigated in the past literature. Subsequently, the effects of PV power on voltage profile and line overload, as well as voltage flicker as a result of cloud movement, in the secondary network are studied. It is observed that flicker in the range of “visible” can occur in the presence of PV power. Finally, a solution based on the differential current is proposed to prevent network protector false trip in the presence of PV power.

In this paper, the terms *secondary network* and *downtown network* are interchangeably used and are the same. The remainder of this paper is organized in the following order: Section II presents the secondary network under study and its modeling details. Microprocessor Network Protector Relay (MNPR) operation and modes are also discussed in this section along with the proposed solution to upgrade network protectors. In Section III, different PV arrangements and allocation methods are provided for simulation purposes. Simulation results regarding trip statistics, cascaded tripping, line overloading, and reclose issues are also discussed here using MNPR. The impacts of using the proposed Smart Network Protector Relay (SNPR) are discussed in Section IV along with simulation results for cloud effects and network voltage profile in the presence of PV power. Finally, concluding remarks are made in Section V.

II. LOW-VOLTAGE SECONDARY NETWORK

The secondary network is the portion of the distribution system between the primary feeders and customer premises where a highly meshed circuit delivers power to the customers

from multiple points to increase reliability (See Fig. 1) [18], [19]. The feeders are connected to one substation to avoid phase angle difference. The reliability and continuity of power is very important in downtown networks due to the nature of the loads and/or population located in those areas. This type of network has been used in the majority of the large cities in the United States since the early 19th century [17]. The traditional low-voltage downtown networks are designed such that the primary substation is the sole source of power. Any reverse power flow towards the primary feeders is an indicator of a fault being fed in the upstream network. Therefore, distributed generation potentially conflicts with network operation due to the possibility of bidirectional power flow.

A. Network Under Study

The selected secondary network is the Warehouse District in the city of New Orleans. The network details are shown in Table I. Secondary network nodes fall into two groups including *grid* network (GN) and *spot* network (SN) that are both connected to the *feeder* network (FN)—also called upstream network—through the network protectors. This network is fed from seven 13.2 kV feeders all connected to the main substation. Feeders are connected to the grid and spot networks through underground grid vaults (GVs) and spot vaults (SVs) where transformers and network protector relays are located. Figure 2 depicts Grid Vault 2 connecting Feeders 1 and 6 to the grid network nodes 20 and 23. A total number of 169 transformers and their corresponding network protectors serve in the secondary network and are all located in the vaults. Out of these transformers 6, were disconnected by the utility company for maintenance and are considered open throughout this study. Each vault is fed from two or more feeders to increase network reliability. Grid network vaults with 120/208V levels serve loads up to 500 kVA (with the exception of two loads) that account for approximately 56% of the network’s loads. Spot vaults with 120/208V or 277/480V

Table I. The secondary network details

Nodes			Lines			Loads amount (pu)			Trans vaults
FN	GN	SN	FN	GN	SN	FN	GN	SN	
409	648	152	408	717	118	0	20.48	13.21	169
						0	7.18	4.62	
1209			1243			P= 33.69MW Q= 11.79MVar			163 in service

Table II. The secondary network loads

Group	Power Range	Number of loads per network		Total
		GN	SN	
Very Large Load	Larger than 1 MVA	1	2	3
Large Load	0.2-1 MVA	31	22	53
Medium Load	50-200 KVA	80	1	81
Small Load	10-50 KVA	57	1	58
Very Small Load	0-10 KVA	33	0	33

†There is no load located on feeder nodes.

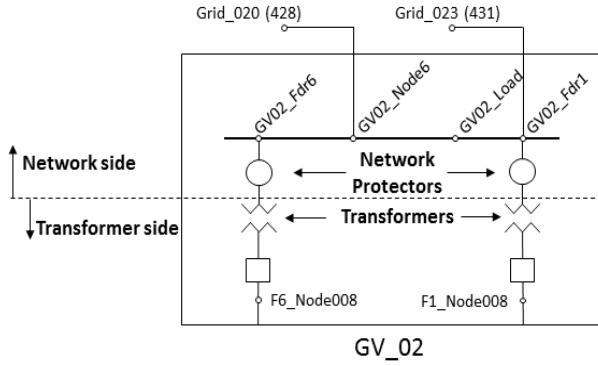


Fig. 2 LV secondary network grid vault connected to two feeders

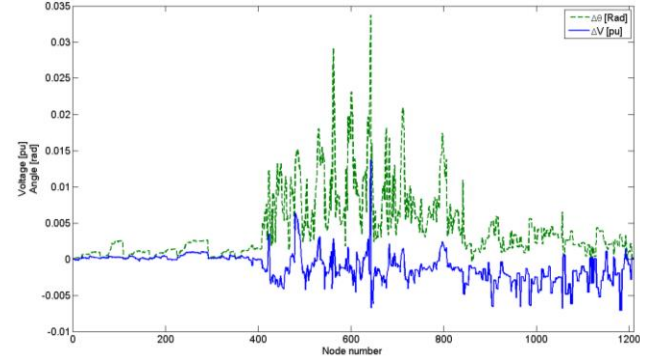


Fig. 3 Simulated network voltage profile mismatch with field

levels serve high-load buildings and heavily loaded nodes up to 1500 kVA. A total of 228 loads are supplied in the selected downtown network as summarized in Table II.

B. Network Model

The downtown network is modeled as a balanced three-phase system. Loads on all network nodes are also three-phase loads. Since the effect of excess power and the proposed solution (discussed later) are not affected by the imbalance that may exist in the network, the balanced three-phase modeling is adequate for the study. Load flow is used to solve the network for steady-state operation using the line impedance model. Nodes that are short distances apart are combined and a reduced network of 928 nodes is obtained. Power flow direction is used to determine the operation status of the network protector relays. Once reverse flow is detected, the pertinent network protector is tripped and load-flow is performed subsequently. A similar scenario is used for the relays' reclose operations. The total network full load is 33.69 MW and 11.79 MVar while the networks minimum load is considered 16% of its full load based on the historical field data (recent minimum load is higher than 16%). Figure 3 depicts the model's voltage profile mismatch when compared to the data provided by the utility company. The figure shows less than 1% mismatch in voltage magnitude and 0.1% in phase angle at normal operation. These are the maximum errors among the 1209 nodes' voltage magnitudes and phase angles as compared to that provided by the utility company.

Steady-state studies reveal potential negative impacts of PV integration in the downtown network, and thus load-flow is found sufficient for this purpose. It is anticipated that by taking the dynamic behavior of the network into account through more detailed simulations, the observed impacts will be slightly larger. Since the objective of this paper is to present the investigation of potential impacts and not detailed simulations necessary for implementation, steady-state simulation is chosen. The transients usually aggravate the predicted problems and detailed time-domain simulations will possibly show additional negative impacts in the study, but will not affect the proposed solution as will be explained.

C. Microprocessor Network Protector Relay (MNPR)

Network protector relays are the key elements in a secondary network protection system. The modern MNPR is a digital relay that combines the functions of a master relay and a network phasing relay. The older types of these MNPR relays (that are still in use) are electro mechanical requiring fine mechanical adjustment to operate. The MNPRs are programmable and have many built-in controls to avoid their ancestor issues such as "ratcheting" [18].

Regular MNPR has five trip and three reclose modes of operation [17]. The commonly used "Sensitive Trip" and "Reclose" modes are modeled in this study. Since the downtown network is powered from multiple points, power can flow into the secondary network from one upstream feeder and exit from it into another upstream feeder feeding a fault. In normal operation, where there are no faults in the upstream network, the power flows from upstream network to the downtown network through all feeders. The MNPRs' primary task is to protect the network against upstream feeder faults. This is done by sensing a reverse power flow through the Sensitive Trip mode. Once a faulty feeder is disconnected from the main substation, the fault in the upstream network is fed by the other feeders through the downtown network. Network protectors sense the reverse power flow from the downtown network to the upstream feeder and disconnect the circuit. The MNPR takes six cycles to trip and an adjustable number of cycles are required to occur for a reclose operation. A reclose time of six cycles is considered in this study. The Sensitive Trip is set to 0.15% of the rated transformer current [24]. The transformer protection will also trip overloaded transformers when the loading exceeds 100% of the transformer rating. It is important to note that the transformer rating is usually higher than the transformer nominal load. Line overload is also considered in this paper by adopting 105% of the line nominal current as the overload limit. It should be noted that the underground downtown distribution lines have lower overload tolerance than their overhead counterparts due to the insulation material of the cables.

The reclose characteristic of the network protector relay is shown in Fig. 4. In the figure, reclosing voltage V_D , which is

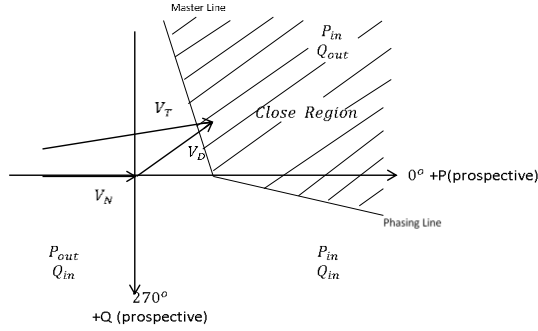


Fig. 4 Reclosing characteristic of the MNPR

the voltage difference between the two sides of the network protector, is observed. That is, $V_D = V_T - V_N$ where V_T is the transformer side voltage and V_N is the voltage on the network side (see Fig. 2). If the fault exists in the upstream circuit, transformer voltage V_T lags or is smaller in magnitude than network voltage V_N . The reclosing action takes place only when the voltage on the transformer side of the open network protector is slightly higher in magnitude and is in-phase with or leading the voltage on the network side of the network protector. The default setting for the reclose voltage is 1.4V (this usually ranges 0.1 to 10.0V).

D. Smart Network Protector Relay (SNPR)

The smart network protector relay is proposed here to prevent the false trip due to reverse power flow caused by excess power inside the network and to allow isolation in the case of an upstream fault. The SNPR operation is similar to a regular network protector in all modes except for the Sensitive Trip mode. In the Sensitive Trip mode a regular MNPR detects a reverse power flow and initiates a trip assuming fault occurrence in the upstream feeder. In the presence of PV units, a regular MNPR does not differentiate between the reverse flow due to an upstream fault and that due to the excess PV power. Available solutions target the power generation from PVs (DGs in general) in order to prevent reverse power flow. These solutions either limit the power generation by PV units to the customer's minimum load consumption, or they require a large communication infrastructure that makes it possible to turn off the PV units by the utility control center when reverse power is detected [7], [23]. This can cause customer complaints and is a waste of available renewable energy, especially when network minimum load is considered. On the other hand, this is not applicable to the currently installed PV units with high capacity (e.g., PV Arrangement 1 explained in the next section). In contrast, by using the SNPR, an algorithm is proposed to detect excess power and override the Sensitive Trip in this case. The proposed protection mechanism does not limit the customers' power generation nor does it need a comprehensive communication infrastructure to communicate with the individual PV units.

Proposed excess power detection method: The proposed method is a *generalized* differential current protection method.

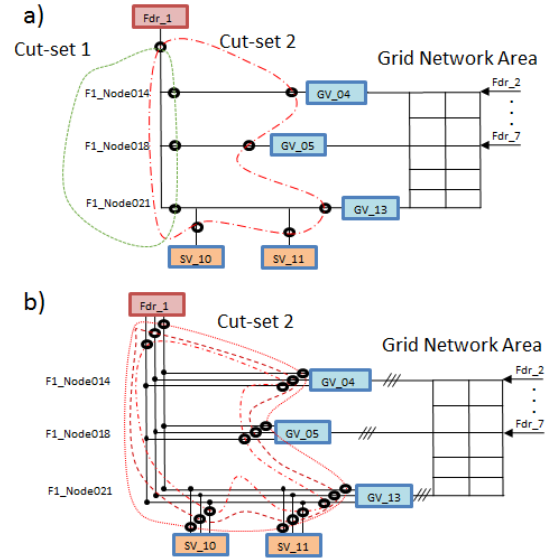


Fig. 5 a) Two instances of closed cut-sets b) Cut-set 2 per-phase structure of the proposed SNPR

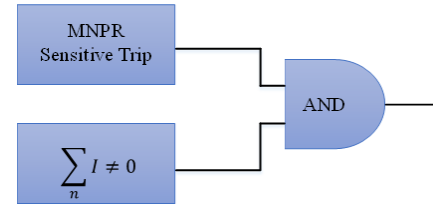


Fig. 6 Smart Network Protector Relay (SNPR) sensitive trip logic

First, a cut-set that surrounds part of the upstream feeder is obtained. This cut-set covers the protected upstream network including the network protectors that separate the feeder network from the secondary network. Two possible cut-sets are depicted as examples in Fig. 5a. These cut-sets cross the feeder lines connected to GV's and SV's as well as the feeder breaker or a feeder line. Ideally, the cut-set encompasses the entire feeder's borders with the secondary network. However, a smaller portion of the feeder can also be chosen to simplify the circuit.

Next, the summation of all measured currents in the selected cut-set is obtained. If the summation is zero, the power only travels through the cut-set; i.e., power flows in the forward or reverse direction through the cut-set with no leak inside the cut-set. If the currents' sum is not zero, power is consumed within the cut-set; i.e., a fault exists in the cut-set. It should be mentioned that the proposed approach is conducted on each phase separately. That is, each phase has a separate cut-set that examines the currents into the cut-set and out of it. Figure 5.b depicts the three-phase representation of Cut-set 2 shown in Fig. 5.a. The signed summation of these currents must add up to zero for safe operation. Upstream load (if any) phase currents are included in the summation. Thus, three-phase current imbalance in the downtown network does not affect the detection mechanism. Selection of the cut-set is critical as it must encompass a feeder or a part of a feeder along the feeder borders that includes network protectors. Also, the interior

nodes must not include loads; that is, the load branches, if there are any in the feeder network, must lie on the cut-set itself (and thus the cut-set is non-planar). In summary, both the reverse power flow and the non-zero cut-set net current signal must exist for a Sensitive Trip to be issued in the proposed SNPR as shown in Fig. 6. The proposed SNPR aims to increase network reliability while being simple as a feasible upgrade for available MNPRs. Communication between the cut-set current measurements are to be performed and the results are transmitted to all the cut-set SNPRs in six cycles for effective operation. Since the proposed mechanism is only applied to the upstream network, a smaller network is targeted, and thus the communications infrastructure is not large and can be as small as a feeder or a part of a feeder.

Many studies have proposed communications infrastructure for control and monitoring of DG units and the distribution network containing them [11]–[15]. However, in the proposed SNPR, communicating with a large number of PV units is not required. Rather, the communications system transmits a small amount of data which is the value of the measured cut-set currents to and from the cut-set control center, that can be one of the SNPRs. Alternatively, the current transformers can be connected in parallel such that the current summation can be physically obtained.

It should also be mentioned that changing the setting of the existing network protectors to allow higher reverse power flow is challenging since high-impedance and single-phase faults, which are low power faults in nature, may be missed and cause damage to the critical downtown underground network. In addition, hourly and intermittent changes of solar power make the relay setting a difficult task.

III. MNPR OPERATION

In this section, detailed studies of MNPR operation are discussed. The solar power generated by the PV panels inside the downtown network cause changes in the feeder and line currents that can lead to network protector false trips and/or line and transformer overloads. In the following discussion different cases of solar and load powers are considered; then, voltage profile and stability as well as line and transformer overloads are studied.

One of the major consequences of the network protector trips is the change in the feeders' injected reactive and active power patterns that may lead to reactive power shortage, in the presence of unity-power factor solar power, followed by voltage instability. As the number of disconnected network protectors increases, network connectivity to the upstream feeder network decreases leading to a less stable downtown network. The effect of the downtown network connectivity on the voltage stability is studied through the lowest eigenvalue of the network Jacobian matrix. Here, all PV units are considered as constant power generations, and thus bus voltages are not controlled. As the minimum eigenvalue approaches zero, the Jacobian matrix approaches singularity and more reactive power support is required to maintain the voltage.

A. PV Arrangements

PV power allocation varies by costumers' locations and interest. It is reasonable to assume that with higher PV penetration, the chances of reverse power flow is increased. The PV power penetration can be either high-generation sites, such as large buildings or large utility-owned solar generators, or distributed PV power generation. In the latter form, one can reasonably assume that the amount of power generation at each node is proportional to the nominal load at that node. Consequently, three PV arrangements are considered in this study and are referred to as Arrangements 1, 2, and 3.

Arrangement 1 (distributed): This arrangement is comprised of distributed PV units across all the downtown network loads. In this arrangement PV units are at 228 loaded nodes. Power of the PV unit at each node in Arrangement 1 is varied from 15% to 150% of the full load of the node. That is, all the PV generators experience 5%, 15%, 30%, 45%, ..., and 150% of their corresponding node's full load, simultaneously.

Arrangement 2 (lump): This arrangement consists of 56 large PV units installed on 56 Large and Very Large Loads (see Table II) in grid and spot networks. Total power of PV in Arrangement 2 is varied from 5% to 150% of the full load of the entire downtown network similar to the previous case. For instance, at 150% penetration, PV Arrangement 2 has a total capacity of 1.5 times the total downtown network full load (33.6 MW); that is, 50.4 MW is distributed among 56 PV units proportional to their corresponding node's load size.

Arrangement 3 (residential): This arrangement contains PV generation on the loads less than 200KW in the grid network, which are 172 loads in this study with a total of 10.12 MW power consumption. In this arrangement, each installed PV unit generates power varying from 5% to 150% of its corresponding node's full load similar to Arrangement 1.

B. MNPR Trip Statistics

The network protector's primary task is to protect the upstream network and transformers. The transformers connect the upstream feeders to the secondary network and are protected against reverse power flow and overload. As the PV penetration level rises, the chances of transformer disconnects due to reverse flow increase. Also, transformer overload can occur if a large share of disconnected transformers is burdened on the connected ones. If all connections to a load are disconnected, the load and its PV generator are removed from the analysis. This is usually the case when a spot network sends power to all of its connected upstream feeders, and thus all its network protectors trip.

The MNPRs are first simulated under hourly load and solar power for different seasons of the year. The solar power measured by the authors, as well as the load profiles provided by the utility company, for the full year of 2015 are utilized here. Figures 7.a and 7.c illustrate load patterns of days with typical and minimum load profile in the summer and winter. Figure 7.b and 7.d present normalized PV power of days with typical and maximum solar power generation in the summer

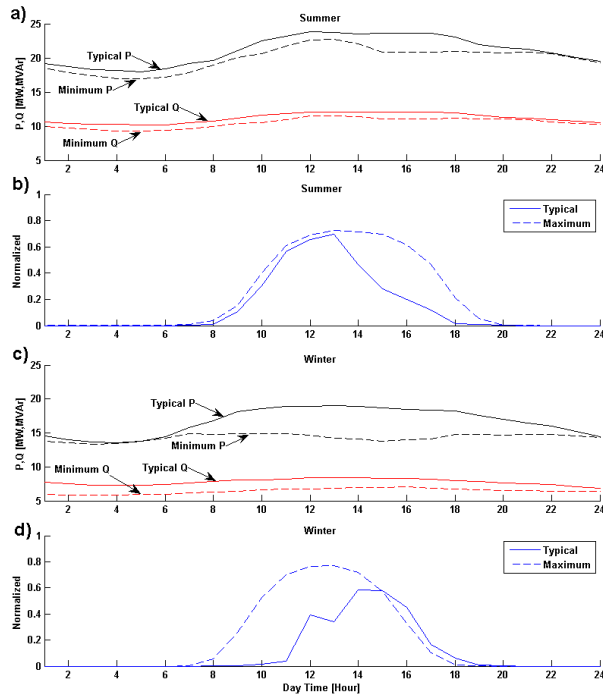


Fig. 7 Seasons: minimum and typical load profiles, maximum and typical PV power. a) Summer days load profile b) Summer days PV power c) Winter days load profile d) Winter days PV power

and winter. The numbers of MNPR trips are presented in Fig. 8 using typical load profile and typical PV power for different scenarios of PV Arrangements 1 and 2 in each season. The PV% in the figure represents the maximum power capacity of individual PV units (that occurs at summer noon time) with respect to their pertinent customer full load. In order to consider the worst case, Fig. 9 presents similar scenarios using minimum

load and maximum PV power for similar arrangements for each season. It is shown in the figures that in the cases where the solar power is greater than that of the load (mostly around noon time) excessive MNPR trips occur, leading to voltage instability in some cases.

In addition, Tables III through V present various solar power penetration and loads statistics independent of the time of the day. Table III shows the number of tripped network protectors (transformers) versus PV penetration levels for Arrangement 1 at the network's historical minimum and full load conditions that are 16% and 100% of the downtown network's full load, respectively. The shaded rows in the table illustrate cases where voltage instability and collapse occur due to reactive power shortage fed by upstream feeders. Recall that PV panels usually operate at unity power factor to increase efficiency, and thus are not sources of reactive power. The emerging smart inverters that are capable of generating reactive power are now under development [25] and study, and their full deployment requires sophisticated control mechanisms along with a comprehensive communication structure. Even with the smart inverters, isolation of the downtown network protector from the upstream feeder network can occur leading to an islanded downtown network. Since all loads are equipped with PV power proportional to their full load demand, the reverse flow does not occur when the PV generation falls below the load demand as shown in Table III. However, when the PV generation exceeds the load demand, both reverse flow and MNPR trips occur in large numbers leading to voltage instability. One outcome of this result is the possibility of voltage collapse around noon when all PV power reserve is in place (as suggested by Figs. 8 and 9). When the system experiences minimum load, the voltage instability occurs at significantly lower PV power levels.

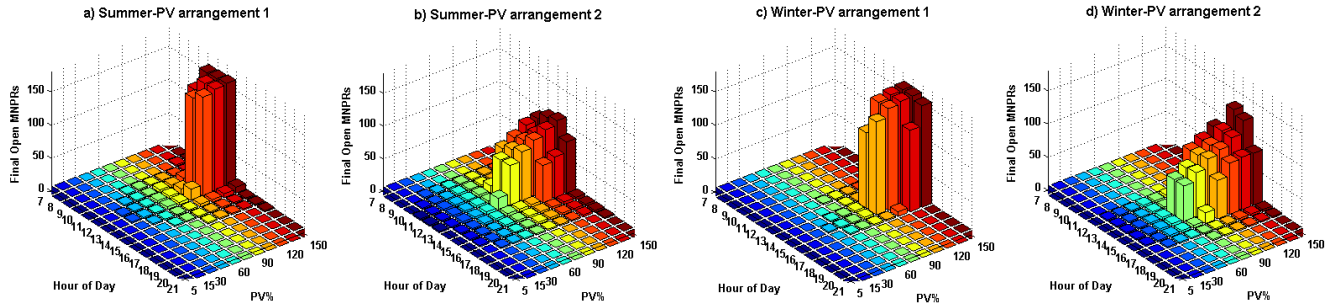


Fig. 8 Number of tripped MNPRs with typical hourly load and typical solar power for different seasons and PV arrangements

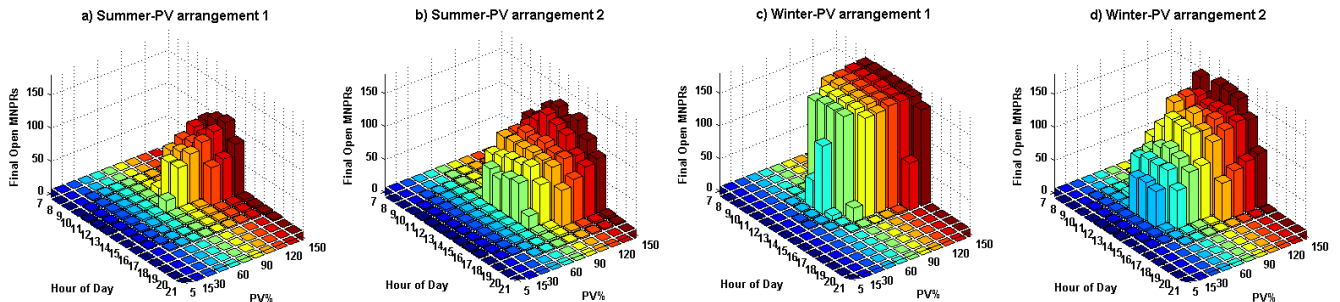


Fig. 9 Number of tripped MNPRs with minimum hourly load and maximum solar power for different seasons and PV arrangements

Table III. MNPR operations in the case: PV Arrangement 1

	Full Load					Minimum Load				
	Trip Incidents				Final	Trip Incidents				Final
PV %	#	R	O	T	F	#	R	O	T	F
5	0	0	0	0	0	0	0	0	0	0
15	0	0	0	0	0	0	0	0	0	0
30	0	0	0	0	0	1	152	0	152	152
45	0	0	0	0	0	1	156	0	156	156
60	3	9	0	9	9	1	157	0	157	157
75	3	8	0	8	8	1	157	0	157	157
90	3	10	0	10	10	1	159	0	159	159
105	1	143	0	143	143	1	159	0	159	159
120	1	155	0	155	155	1	159	0	159	159
135	1	157	0	157	157	1	159	0	159	159
150	1	157	0	157	157	1	159	0	159	159

*#: rounds of cascaded trips, R: trip due to reverse flow, O: trip due to overload, T: Total number of trip incidents, F: Final open MNPRs

Table IV. MNPR operations in the case: PV Arrangement 2

	Full Load					Minimum Load				
	Trip Incidents				Final	Trip Incidents				Final
PV %	#	R	O	T	F	#	R	O	T	F
5	0	0	0	0	0	1	1	0	1	1
15	1	1	0	1	1	6	81	0	71	71
30	1	2	0	2	2	>20	508	0	152	133
45	1	2	0	2	2	>20	584	2	157	132
60	1	3	0	3	3	1	152	0	152	152
75	3	83	0	83	58	1	154	0	154	154
90	>20	214	0	214	68	1	156	0	156	156
105	5	95	0	95	83	1	156	0	156	156
120	>20	208	1	209	81	1	156	1	157	157
135	>20	422	0	422	96	1	146	11	157	157
150	15	497	9	506	111	1	146	11	157	157

*#: rounds of cascaded trips, R: trip due to reverse flow, O: trip due to overload, T: Total number of trip incidents, F: Final open MNPRs

Tables IV and V illustrate the trip statistics when Arrangements 2 and 3 are adopted. In Table IV, when PV power penetration level is 150% (of full load) at network full load condition, 395 incidents of reclose occur in 15 rounds of cascaded trip incidents leading to a final 111 tripped MNPRs at which point the network voltage stability is undermined. In the cascaded trips, several rounds of trips and/or reclose operation occur before the network settles down to a steady configuration. One round of MNPR trips pushes the extra power towards other network protectors and causes a separate round of trips in other network protectors and/or causes some of the tripped MNPRs to reclose. This may repeat a few times before the network comes to a final configuration as shown in Table IV. This phenomenon may lead to *pumping* (which happens more severely with Arrangements 2 and 3). In addition, MNPR trip incidents leave lower paths for extra power to flow toward the upstream network or for demanded power to flow towards loads. As the excess power is guided through fewer numbers of

Table V. MNPR operations in the case: PV Arrangement 3

	Full Load					Minimum Load				
	Trip Incidents				Final	Trip Incidents				Final
PV %	#	R	O	T	F	#	R	O	T	F
5	0	0	0	0	0	0	0	0	0	0
15	0	0	0	0	0	0	0	0	0	0
30	0	0	0	0	0	>20	275	0	275	51
45	1	1	0	1	1	>20	460	0	460	79
60	1	1	0	1	1	>20	436	2	438	81
75	1	1	0	1	1	>20	478	6	484	76
90	1	1	0	1	1	1	94	0	94	94
105	1	1	0	1	1	1	96	0	96	96
120	2	4	0	4	4	1	96	0	96	96
135	3	10	0	10	9	1	96	0	96	96
150	>20	98	0	98	21	1	96	0	96	96

*#: rounds of cascaded trips, R: trip due to reverse flow, O: trip due to overload, T: Total number of trip incidents, F: Final open MNPRs

Table VI. Voltage stability metrics for cases with PV Arrangement 3

PV%	Full Load		Minimum Load	
	Minimum Eigenvalue	Average Q per NPs [pu]	Minimum Eigenvalue	Average Q per NPs [pu]
5	0.21	0.0683	0.22	0.010
15	0.21	0.0679	0.22	0.010
30	0.21	0.0672	0.09	0.013
45	0.21	0.0669	4.2e-15	0.017
60	0.21	0.0664	5.0e-15	0.018
75	0.21	0.0660	0.08	0.019
90	0.21	0.0656	-8.9	0.020
105	0.21	0.0653	-21.45	0.021
120	0.10	0.0662	-163.3	0.022
135	0.10	0.0678	-20.52	0.023
150	0.16	0.0731	-2.1	0.024

transformers, the chance of transformer overload increases and additional trips due to overload occur.

With Arrangement 3, the total PV power generation is lower than with the other two arrangements, and thus PV generation is never higher than the downtown network's full load. Consequently, voltage instability does not occur in the case with full load. As the network experiences the minimum load, one can expect a large number of MNPR trips and voltage instability at higher penetration levels than in Arrangement 1 as shown in Table V. In several PV power levels with Arrangement 3, a number of cascaded trips occur that involve reclose actions. At the network minimum load, when PV power is between 30% and 75%, the number of trip-reclose incidents is significantly high and pumping occurs.

Next, the voltage stability metric introduced earlier is shown in Table VI for Arrangement 3. One can observe that as the number of false trips increases, the feeder network's average reactive power injection through the remaining connected transformers increases and the smallest eigenvalue approaches zero. The negative eigenvalue occurs where

Table VII. Overloaded network lines in different cases

	PV Arrangement 1		PV Arrangement 2		PV Arrangement 3	
PV%	Full load	Min load	Full load	Min load	Full load	Min load
5	0	0	8	0	16	0
15	0	0	44	35	38	5
30	0	n/a	72	96	48	34
45	0	n/a	89	188	60	118
60	0	n/a	99	n/a	70	121
75	0	n/a	132	n/a	75	185
90	0	n/a	139	n/a	81	n/a
105	n/a	n/a	221	n/a	90	n/a
120	n/a	n/a	239	n/a	109	n/a
135	n/a	n/a	301	n/a	115	n/a
150	n/a	n/a	n/a	n/a	151	n/a

Table VIII. SNPR operation for the case with 120% PV penetration and minimum load in PV arrangement 2

Without fault [pu]×10 ⁻²		With fault [pu]×10 ⁻²	
S1: +17.16-j1.28	S2: +0.70+j0.31	S1: +17.22-j1.29	S2: +0.7+j0.31
S3: +5.92-j2.13	S4: +73.60-j5.25	S3: +5.92-j2.14	S4: +73.84-j5.27
S5: +10.30-j1.61	S6: +18.87-j1.69	S5: +10.33-j1.62	S6: +18.90-j1.71
S7: +6.41-j2.44	S8: +4.90-j2.35	S7: +6.41-j2.45	S8: +4.89-j2.36
S9: +3.88-j1.28	S10: +24.00-j1.00	S9: +3.89-j1.28	S10: +24.08-j1.00
S11: +45.77-j3.35	S12: +5.49-j1.62	S11: +45.92-j3.36	S12: +5.55-j1.62
S13: +11.92-j2.33	S14: +43.12-j2.87	S13: +11.91-j2.36	S14: +43.25-j2.88
S15: +31.09-j1.33	S16: +48.07-j3.54	S15: +31.17-j1.34	S16: +48.18-j3.56
S17: +53.78-j3.21	S18: +11.45-j1.79	S17: +53.89-j3.24	S18: +11.48-j1.80
S19: +1.30-j0.61	S20: +7.00-j1.10	S19: +1.30-j0.61	S20: +7.00-j1.11
S21: +38.39-j0.68	S22: +25.62-j0.62	S21: +38.50-j0.68	S22: +25.70-j0.62
S23: +26.48-j0.73	S24: +8.32-j2.17	S23: +26.58-j0.73	S24: +8.34-j2.18
S0: -522.99+j45.73		S0: -522.78+j45.94	
Sum: +0.53+j1.05		Sum: +2.13+j1.05	

network voltage collapse is predicted by Table V for this arrangement. The other Arrangements show similar behavior but are not shown here due to lack of space.

C. Distribution Line Overload Statistics

The PV generation inside the downtown network may affect the distribution lines' loading and cause them to overload. The number of overloaded lines in the network increases with the PV power. Table VII summarizes the distribution line overload incidents as a function of PV power level for Arrangements 1, 2, and 3 at full and minimum loads. As predicted, with distributed PV power generation the likelihood of line overload is lower. Here, the overload level is considered as 105% of the underground line current at the downtown network full load condition when no PV generation exists in the network. This result is conservative in the sense that the actual overload capability of the distribution lines may be higher in the actual

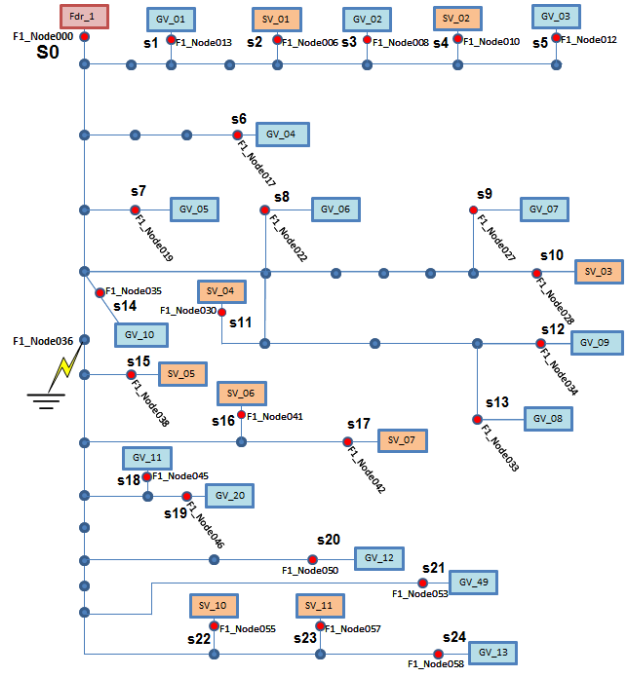


Fig. 10 Node 562 voltage variations due to cloud

network. However, this data was not available. Also, no line disconnect is assumed due to overload since the loadability of individual lines were not known.

D. MNPR Reclose operation

The default reclose voltage setting of the relay simulated in this study is 1.4V ($V_D=1.4V$) [24]. The relay reclose voltage setting establishes the minimum difference voltage required to issue a reclose command when the feeder voltage and network voltage are in phase. With the default reclose setting, a number of network protectors that are tripped due to reverse power flow will reclose after the reclose cycle has passed. A solar power penetration scenario is arranged to show the pumping effect. At the MNPR in Grid Vault 29 fed by Feeder 4, the voltage difference is $V_D = 1.87V > 1.4V$; and at the MNPR in Grid Vault 44 fed by Feeder 7, $V_D = 1.62V > 1.4V$ after the trip due to reverse power flow. Thus, the two network protectors in the vaults are ready to reclose. However, after MNPRs reclosed, both transformers see reverse power again and subsequently trip. This process will continue leading to excessive relay operations which is known as *pumping* [20]. Allowing the network protector to close with a small difference voltage magnitude can lead to pumping in certain arrangements and penetration levels as observed. However, it can be seen that when the threshold is increased to 2V, pumping does not occur when the MNPR is used. As expected, pumping due to reverse power does not occur when SNPR is utilized in either reclose setting case illustrated.

IV. CASE STUDIES FOR SNPR

The results obtained in previous sections indicate network protector false operations in the presence of PV power generation inside the network. Currently, the network

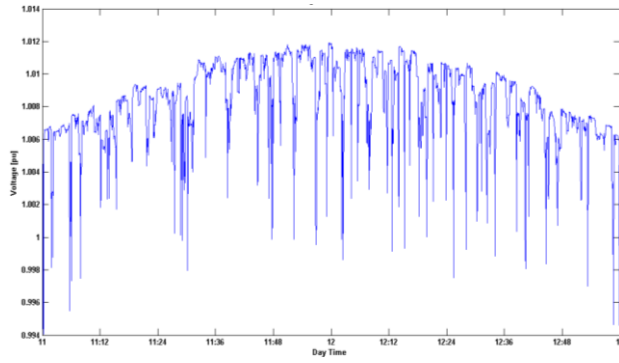


Fig. 11 Node 562 voltage variations due to cloud

protectors can't differentiate between PV excess power flow and an upstream fault. That is, the network protectors trip the circuit once they sense a reverse flow regardless of its cause. The MNPR false trip can destabilize the network as discussed in the previous section.

The idea of a smart network protector was explained earlier in Section II. Here, the smart network protector is applied by upgrading regular network protectors with an overriding logic. This overriding logic prevents false tripping when reverse flow is originated from PV excess power generation in downstream branches. Thus, in the case where there is no fault in the upstream feeder with reverse flow, the smart network protector avoids circuit disconnection. Consequently, it is expected that no trips occur unless transformer overload limits are reached. Here, the PV Arrangement 2 with 120% PV penetration is considered (from Table IV) and Feeder 1 is selected to show the operation of the SNPR in differentiating between an upstream fault and PV excess power. Figure 10 presents the topology of feeder 1 where a cut-set similar to that of Fig. 5 crosses all of the upstream boarder nodes (nodes depicted in red). Under normal operation, the summation of the currents from all the vaults is equal to that of the main breaker considering no line losses. These values are given in Table VIII where positive currents represent current directions into the cut-set. It is shown that the sum of the signed currents equals $0.0053 + j0.0105$ under the PV excess power; a small value that indicates excess power only. Next, a three-phase high-impedance fault of 0.1 p.u (power) is introduced in the upstream Feeder 1 on node F1_Node036 as depicted in Fig. 10. This time the currents of the feeder cut-set sum up to $0.0213 + j0.0105$. This larger current summation is an indicator of an upstream fault. Thus, the SNPRs observing reverse power (all Feeder 1 SNPRs according to Table VIII) are allowed to trip.

Cloud Effect

The intermittent nature of PV power causes injected power variations at downtown network nodes. In this research, scattered cloud movement effects are considered by randomly assigning power drop at PV generation locations throughout the secondary network at high PV power levels. In order to generate the random power, solar power was measured over a course of twelve months in 2015 at Louisiana State University.

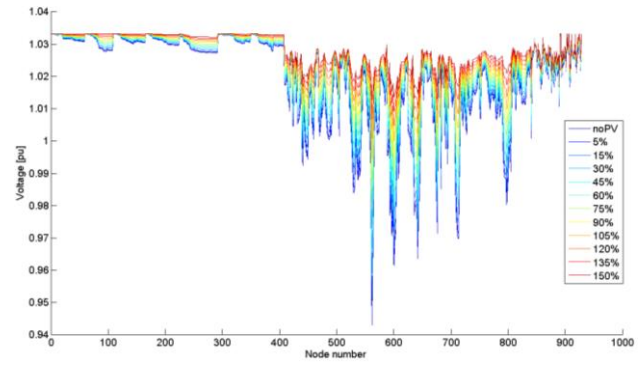


Fig. 12 Network's voltage profile during full load

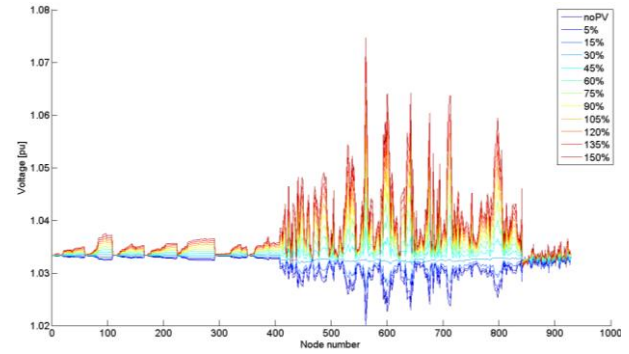


Fig. 13 Network's voltage profile during minimum load

After investigating the measured data in all seasons, winter (where solar power variation is significant) is chosen for cloud discussions. The PV power is measured through a 140-Watt solar panel connected to a resistive load. A Fluke-43B data acquisition system is used, along with LabVIEW software, to capture the voltage every four seconds. One of the days in winter with the most PV power variation is chosen and the maximum power level fall and duration are obtained. Then the cloud assignment is determined by considering $T_{up} = -a \times \ln U_1$ and $T_{down} = -b \times \ln U_2$ where U_1 and U_2 are uniformly distributed random numbers in the range $[0,1]$ and a and b are average up and down times in the solar irradiation. The power drop is generated through a uniformly distributed random number in the range of zero to 60% solar irradiance drop. Subsequently, 228 random variable power levels are generated using the random distribution functions explained above and are applied to all load nodes in Arrangement 1 at 100% (of full load) penetration level. At this level, no reverse power is observed by MNPRs, and thus no MNPR trips occur. It is observed that at some nodes, voltage flicker in the range of "visible" occurs as shown in Fig. 11 based on IEEE 519 definitions [21]. With the SNPR and higher PV power levels, voltage flicker increases. Higher penetration of the solar power in the downtown network causes more power fluctuations due to cloud movements, and thus more flicker is observed in the downtown network.

Voltage Profile

DG has been shown to affect the voltage profile in secondary networks [4], [9], [22]. Voltage analysis of the selected downtown network under full and minimum loading in

the presence of different PV generation is discussed in this section for Arrangement 1. Different penetration levels of PV power are considered at loaded nodes that range from 15% to 150% of the nodes' full load. The networks voltage profiles are presented in Figs. 12 and 13. It is shown in the figures that the chances of overvoltage are high in the minimum load condition under high penetration levels. The voltage profiles are obtained by considering SNPRs to allow higher penetration levels. With the MNPR, the voltage profiles are very similar up to the point of voltage collapse where no voltage is established.

V. Conclusion

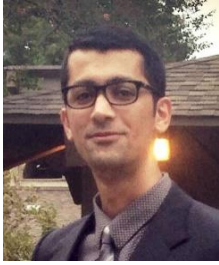
Operational challenges of network protectors in downtown networks in the presence of PV power integration are discussed in this paper. A model is developed for the downtown network based on line impedance models, and load flow is performed to simulate the network operation. Distributed PV unit arrangements are utilized and the results are compared. It is demonstrated that large network protector trips can occur in the presence of PV power leading to potential network voltage collapse. Smart network protectors that distinguish between upstream faults and PV excess power are proposed, and network operation is compared with and without the smart network protectors. Finally, voltage profile and flicker are shown to be affected by the PV power installed in the downtown network.

VI. Acknowledgement

We express our appreciation to the Entergy of Louisiana, distribution team Mark Bruckner, Tom Field, David Chemin, Jim Dean, Randall Roberts, and Michael Gray for their support and encouragement throughout this work.

REFERENCES

- [1] Katiraei, F.; Agüero, J.R., "Solar PV Integration Challenges," *Power and Energy Magazine, IEEE*, vol.9, no.3, pp.62,71, May-June 2011.
- [2] Walling, R.A.; Saint, R.; Dugan, R.C.; Burke, J.; Kojovic, L.A., "Summary of Distributed Resources Impact on Power Delivery Systems," *Power Delivery, IEEE Transactions on*, vol.23, no.3, pp.1636,1644, July 2008.
- [3] U.S. Solar Market Insight Report, Q1 2015, executive summary. [Online] Available: <http://www.seia.org/research-resources/solar-market-insight-report-2015-q1>
- [4] Po-Chen Chen; Salcedo, R.; Qingcheng Zhu; de Leon, F.; Czarkowski, D.; Zhong-Ping Jiang; Spitsa, V.; Zabar, Z.; Uosef, R.E., "Analysis of Voltage Profile Problems Due to the Penetration of Distributed Generation in Low-Voltage Secondary Distribution Networks," *Power Delivery, IEEE Transactions on*, vol.27, no.4, pp.2020,2028, Oct. 2012.
- [5] Ochoa, L.F.; Harrison, G.P., "Minimizing Energy Losses: Optimal Accommodation and Smart Operation of Renewable Distributed Generation," *Power Systems, IEEE Transactions on*, vol.26, no.1, pp.198,205, Feb. 2011.
- [6] Brown, T., "Transmission network loading in Europe with high shares of renewables," *Renewable Power Generation, IET*, vol.9, no.1, pp.57,65, 1 2015.
- [7] Tonkoski, R.; Lopes, L.A.C.; El-Fouly, T.H.M., "Coordinated Active Power Curtailment of Grid Connected PV Inverters for Overvoltage Prevention," *Sustainable Energy, IEEE Transactions on*, vol.2, no.2, pp.139,147, April 2011.
- [8] Hooshyar, H.; Baran, M.E., "Fault Analysis on Distribution Feeders With High Penetration of PV Systems," *Power Systems, IEEE Transactions on*, vol.28, no.3, pp.2890,2896, Aug. 2013.
- [9] Baran, M.E.; Hooshyar, H.; Zhan Shen; Huang, A., "Accommodating High PV Penetration on Distribution Feeders," *Smart Grid, IEEE Transactions on*, vol.3, no.2, pp.1039,1046, June 2012.
- [10] Cheung, H.; Hamlyn, A.; Lin Wang; Cungang Yang; Cheung, R., "Investigations of impacts of distributed generations on feeder protections," *Power & Energy Society General Meeting, 2009. PES '09. IEEE*, vol., no., pp.1,7, 26-30 July 2009.
- [11] Yazdanpanahi, H.; Yun Wei Li; Wilsun Xu, "A New Control Strategy to Mitigate the Impact of Inverter-Based DGs on Protection System," *Smart Grid, IEEE Transactions on*, vol.3, no.3, pp.1427,1436, Sept. 2012.
- [12] Alam, M.J.E.; Muttaqi, K.M.; Sutanto, D., "Mitigation of Rooftop Solar PV Impacts and Evening Peak Support by Managing Available Capacity of Distributed Energy Storage Systems," *Power Systems, IEEE Transactions on*, vol.28, no.4, pp.3874,3884, Nov. 2013.
- [13] Alam, M.J.E.; Muttaqi, K.M.; Sutanto, D., "An Approach for Online Assessment of Rooftop Solar PV Impacts on Low-Voltage Distribution Networks," *Sustainable Energy, IEEE Transactions on*, vol.5, no.2, pp.663,672, April 2014.
- [14] Zamani, M.A.; Yazdani, A.; Sidhu, T.S., "A Communication-Assisted Protection Strategy for Inverter-Based Medium-Voltage Microgrids," *Smart Grid, IEEE Transactions on*, vol.3, no.4, pp.2088,2099, Dec. 2012.
- [15] Schweitzer, E.O.; Finney, D.; Mynam, M.V., "Applying radio communication in distribution generation teleprotection schemes," *Protective Relay Engineers, 2012 65th Annual Conference for*, vol., no., pp.310,320, 2-5 April 2012.
- [16] Li Yu; Czarkowski, D.; De Leon, F.; Bury, W., "A time sequence load-flow method for steady-state analysis in heavily meshed distribution network with DG," *Compatibility and Power Electronics (CPE), 2013 8th International Conference on*, vol., no., pp.25,30, 5-7 June 2013.
- [17] Wei-Jen Lee; Cultrera, J.; Maffetone, T., "Application and testing of a microcomputer-based network protector," *Industry Applications, IEEE Transactions on*, vol.36, no.2, pp.691,696, Mar/Apr 2000.
- [18] IEEE Application Guide for IEEE Std 1547(TM), IEEE Standard for Interconnecting Distributed Resources with Electric Power Systems," *IEEE Std 1547.2-2008*, vol., no., pp.1,217, April 15 2009.
- [19] IEEE Recommended Practice for Protection and Coordination of Industrial and Commercial Power Systems (IEEE Buff Book)," *IEEE Std 242-2001 (Revision of IEEE Std 242-1986) [IEEE Buff Book]*, vol., no., pp.1,710, Dec. 17 2001.
- [20] IEEE Standard Requirements for Secondary Network Protectors," *IEEE Std C57.12.44-2014 (Revision of IEEE Std C57.12.44-2005)*, vol., no., pp.1,65, June 13 2014.
- [21] IEEE Recommended Practices and Requirements for Harmonic Control in Electrical Power Systems," *IEEE Std 519-1992*, vol., no., pp.1-112, April 9 1993.
- [22] Salcedo, R.; Xuanchang Ran; De Leon, F.; Czarkowski, D.; Spitsa, V., "Long Duration Overvoltages due to Current Backfeeding in Secondary Networks," *Power Delivery, IEEE Transactions on*, vol.28, no.4, pp.2500,2508, Oct. 2013.
- [23] NREL Technical Report, "Interconnecting PV on New York City's Secondary Network Distribution System", NREL/TP-7A2-46902, November 2009. Available: www.energy.gov/eere/sunshot/downloads/interconnecting-pv-nycs-secondary-network-distribution-system
- [24] ETI MNPR FieldPro Manual. Available: <http://www.eti-nj.com/support.html>
- [25] EPRI report, "Modeling High-Penetration PV for Distribution Interconnection Studies"
- [26] <http://www.renewableenergyworld.com/rea/news/article/2014/02/the-interconnection-nightmare-in-hawaii-and-why-it-matters-to-the-u-s-residential-pv-industry?cmpid=SolarNL-Thursday-February13-2014>



Pooria Mohammadi (S'15) received his B.S. degree in electrical engineering from Iran University of Science and Technology (IUST), Tehran, Iran, in 2010 and his M.S. degree focused in power system and protection from University of Texas at Tyler, Texas, in 2013.

Currently, he is a Ph.D. candidate at the ECE department, Louisiana State University (LSU). His current research includes power system protection, Optimal PMU Placement (OPP), observability and state estimation, and Distributed Generations (DGs) integration. He has conducted several projects for utility companies during his education and holds three patents. His research interests also include smart grids, renewable energies, PMU applications, intelligent and adaptive methods in power systems, and storage devices.



Shahab Mehraeen (S'08–M'10) received the B.S. degree in electrical engineering from Iran University of Science and Technology, Tehran, Iran, in 1995, the M.S. degree in electrical engineering from Esfahan University of Technology, Esfahan, Iran, in 2001, and the Ph.D. degree in electrical engineering from Missouri University of Science and Technology, Rolla, in 2009. He joined the Louisiana State University, Baton Rouge, LA, USA, as an Assistant Professor in 2010. His current research interests include

micro grids, renewable energies, power systems dynamics, protection, and smart grids. In addition, he conducts research on decentralized, adaptive, and optimal control of dynamical systems. Shahab Mehraeen is a National Science Foundation CAREER awardee and holds a U.S. patent on energy harvesting.